DVS-Net: Dual-domain Variable Splitting Network for Accelerated Parallel MRI Data

Rui Ding[1] and Joseph Bartlett[2] and Jinming Duan[2] and Yuping Duan[1]

***Abstract*— Parallel imaging is an important method to accelerate the acquisition of magnetic resonance imaging data, which can shorten the breath-hold times and reduce motion artifacts. In this paper, we propose a joint frequency domain and image domain (dual-domain) reconstruction method by introducing the full sampling condition for the undersampled multi-coil MR data. The motivation is that the dual domain method can provide more information for accurate image reconstruction. An efficient iterative algorithm is developed based on the variable splitting technique and alternating direction method of multipliers, which is unrolled into an end-to-end trainable deep neural network. We evaluate the proposed network on complex valued multi-coil knee images for both 6-fold and 8-fold acceleration factors, and compare with both variational and deep learning based reconstruction algorithms. The numerical results demonstrate that our method provides better reconstruction accuracy and perceptual quality by making using of the dual domain information.**

***Clinical relevance:* This improves the reconstruction quality for accelerated parallel MRI data both visually and quantitatively.**

I. INTRODUCTION

Magnetic Resonance Imaging (MRI) is an important medical imaging modality, which has been used for both anatomical and functional usage. However, it suffers from a long acquisition time to scan the full k-space data, which not only results in motion artifacts, but also limits the availability of MR scanner for users. Parallel MRI (p-MRI) [1] uses an array of receiver coils to collect undersampled k-space data to reconstruct full FOV images for accelerating the acquisition of MRI data. P-MRI and compressed sensing [15], [16] methods are widely used in imaging problems.

As a matter of fact, the k-space data contains plenty of spatial frequency information. Eo *et al.* [2] developed the KIKI-net for reconstructing undersampled MR images, which consists of three components KCNN for k-space completion, ICNN for removing artifacts and restoring image details, and IDC for regularizing and activating network learning. Souza, Lebel and Frayne [3] proposed a hybrid dual domain cascade of convolutional neural networks intercalated with data consistency layers, which is trained end-to-end for compressed sensing reconstruction of MR images. Model based learning methods have been studied for MRI reconstruction during last several years, and achieved great success in building up efficient network architectures [8], [9], [14]. Based on the general CS p-MRI model, Duan *et al.* [10] established VS-Net through variable splitting method. Jun *et al.* [13] proposed a model-based joint reconstruction network for MR images and coil sensitivities. Note that the aforementioned approaches are investigated on the single-coil acquisition setting, and the multi-coil acquisition data can accelerate the imaging process.

Lin *et al.* [4] proposed an end-to-end trainable dual domain network to simultaneously restore sinogram consistency and CT images, which works well for CT metal artifact reduction. Similar idea has been utilized to recover k-space and images for fast MRI with a deep T1 prior [5]. The full sampling condition has been developed for joint spatial and Radon domain reconstruction for computed tomography (CT) reconstruction [6], [7], which successfully improved the reconstruction quality for both sparse-view and limited angle data. These studies demonstrate that dual domain strategy can complement image domain information effectively.

The successes of both model-based approaches and dual domain strategies provide the impetus for the establishment of our model. More specifically, we propose a novel variational joint dual-domain reconstruction model for accelerated p-MRI problem. The operator splitting and Alternating Direction Method of Multipliers (ADMM) based algorithm are developed for solving the proposed minimization problem, which is handled by end-to-end trainable deep neural networks via deep unrolling strategy. We evaluate the Dual-domain Variable Splitting Network (DVS-Net) on the public dataset and testify the importance of dual-domain information for parallel MRI reconstruction.

II. OUR APPROACH

Let $m \in \mathbb{C}^N$ be a complex-valued MR image, $f \in \mathbb{C}^N$ be the k-space data corresponding to m, $y_i \in \mathbb{C}^M$ be the undersampled k-space data measured from the ith MR receiver coil, and n_c be the total number of receiver coils. It is straightforward to use following model to estimate the MR image for accelerated p-MRI problem

$$\min_m \ \frac{\lambda}{2} \sum_{i=1}^{n_c} \|\mathcal{D}\mathcal{F}S_i m - y_i\|_2^2 + \mathcal{R}_I(m), \tag{1}$$

where $\mathcal{D} \in \mathbb{R}^{M\times N}$ denotes the sampling matrix, $\mathcal{F} \in \mathbb{C}^{N\times N}$ denotes the Fourier transform, $S_i \in \mathbb{C}^{N\times N}$ denotes the i-coil sensitivity, $\mathcal{R}_I(\cdot)$ is the regularization term of image data, and λ is a positive constant used to balance

*The work was supported by National Natural Science Foundation of China (NSFC 12071345, 11701418), Major Science and Technology Project of Tianjin 18ZXRHSY00160 and Recruitment Program of Global Young Expert.

[1]Center for Applied Mathematics, Tianjin University, China, Tianjin, 300072, China yuping.duan@tju.edu.cn

[2]School of Computer Science, University of Birmingham, Edgbaston, Birmingham B15 2TT, United Kingdom

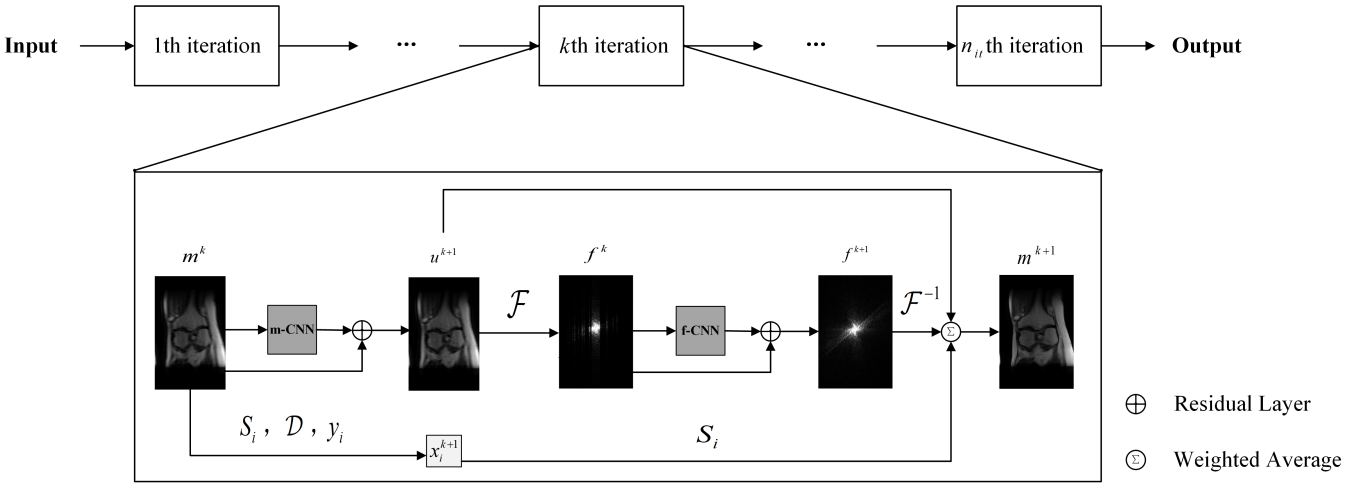

Fig. 1: The end-to-end network structure guided by the dual-domain variable splitting algorithm, where the kth iteration is displayed in details as an example.

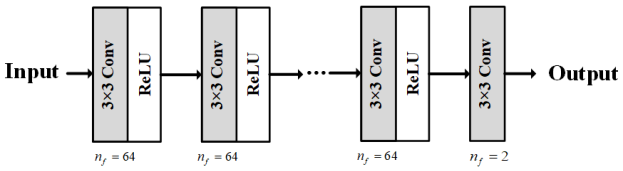

Fig. 2: The CNN block with convolution and activation layers.

between the regularization term and data fidelity term. In [10], the above model was formulated into an alternating direction algorithm and solved by an end-to-end trainable deep neural network, which achieved great success compared to traditional and learning-based reconstruction methods. However, the consistency between frequency domain and image domain is ignored. Thus, we propose a novel dual-domain reconstruction model for accelerated parallel MR problem as follows

$$\begin{aligned}\min_{m,f} \quad & \frac{\lambda}{2}\sum_{i=1}^{n_c}\|\mathcal{D}\mathcal{F}S_i m - y_i\|_2^2 + \mu\mathcal{R}_I(m) + \mathcal{R}_K(f) \\ & + \frac{\gamma}{2}\|f - \mathcal{F}m\|_2^2,\end{aligned} \tag{2}$$

where $\mathcal{R}_K(\cdot)$ denotes the regularization term of k-space data, μ, γ are positive constants, and the L^2 term is used to boost the consistency of between the frequency domain and image domain data. In the followings, we use the variable splitting method to reformulate the above minimization and built up an alternating direction algorithm to solve the dual domain reconstruction model. More specifically, we introduce auxiliary variables u and x_i, $i = 1, \ldots, n_c$, and rewrite the dual-domain model (2) as a constrained minimization problem

$$\begin{aligned}\min_{m,f,u,x_i} \quad & \frac{\lambda}{2}\sum_{i=1}^{n_c}\|\mathcal{D}\mathcal{F}x_i - y_i\|_2^2 + \mu\mathcal{R}_I(u) + \mathcal{R}_K(f) \\ \text{s.t.,} \quad & f = \mathcal{F}m,\ m = u,\ x_i = S_i m.\end{aligned} \tag{3}$$

Based on the penalty method, we can obtain the unconstrained multi-variable minimization problem as follows

$$\begin{aligned}&\min_{m,f,u,x_i} \frac{\lambda}{2}\sum_{i=1}^{n_c}\|\mathcal{D}\mathcal{F}x_i - y_i\|_2^2 + \mu\mathcal{R}_I(u) + \mathcal{R}_K(f) \\ &+ \frac{\alpha}{2}\sum_{i=1}^{n_c}\|x_i - S_i m\|_2^2 + \frac{\beta}{2}\|u - m\|_2^2 + \frac{\gamma}{2}\|f - \mathcal{F}m\|_2^2,\end{aligned}$$

where $\alpha, \beta \geq 0$ are penalty weights. We then implement the ADMM to solve the above minimization problem by splitting it into the following four sub-minimization problems

$$\begin{cases}\min\limits_{x_i} \ \frac{\lambda}{2}\sum_{i=1}^{n_c}\|\mathcal{D}\mathcal{F}x_i - y_i\|_2^2 + \frac{\alpha}{2}\sum_{i=1}^{n_c}\|x_i - S_i m^k\|_2^2, \\ \min\limits_{u} \ \frac{\beta}{2}\|u - m^k\|_2^2 + \mu\mathcal{R}_I(u); \\ \min\limits_{f} \ \frac{\gamma}{2}\|f - \mathcal{F}m^k\|_2^2 + \mathcal{R}_K(f); \\ \min\limits_{m} \ \frac{\alpha}{2}\sum_{i=1}^{n_c}\|x_i^{k+1} - S_i m\|_2^2 + \frac{\beta}{2}\|u^{k+1} - m\|_2^2 \\ \qquad + \frac{\gamma}{2}\|f^{k+1} - \mathcal{F}m\|_2^2.\end{cases}$$

Now we discuss the solutions to the sub-minimization problems. Both u-subproblem and f-subproblem are composed of a data fidelity term and a regularization term, which can be solved as follows

$$u^{k+1} = (\beta I + \mu\partial R_I)^{-1}(\beta m^k), \tag{4}$$

and

$$f^{k+1} = (\gamma I + \partial R_K)^{-1}(\gamma\mathcal{F}m^k), \tag{5}$$

respectively, where I denotes the identity operator. Instead of hand-craft regularization terms, we use neural networks to learn suitable regularization term for both variables u and f. On the other hand, both x_i and m can be solved by the closed-form solutions. Then we summarize the algorithm for solving our joint dual domain reconstruction (2) in below. Note that we directly use u^{k+1} to update f^{k+1} supposing the constraint $m = u$ holds unconditionally, which can help to speed up the convergence.

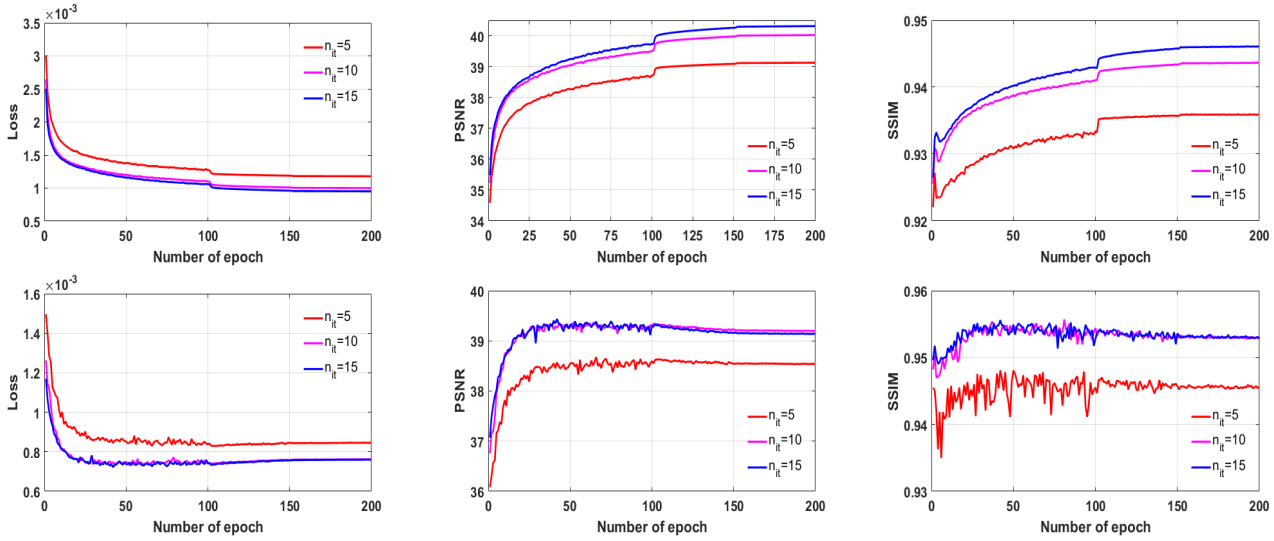

(a) Loss (b) PSNR (c) SSIM

Fig. 3: The curves of three quantitative indicators(Loss, PSNR, SSIM) with the number of epoch during training and testing. The three curves in each picture are curves under three different iterations. The first row is on the training set, and the second row is on the test set.

The Dual-domain Variable Splitting Algorithm

1: Initialize u^0, f^0, m^0, x_i^0 for $i = 1, \ldots, n_c$;
2: **for** $k = 1, \ldots, n_{it}$, **do**
3: $x_i^{k+1} \leftarrow \mathcal{F}^{-1}\big((\alpha I + \lambda \mathcal{D}^T \mathcal{D})^{-1}(\alpha \mathcal{F} S_i m^k + \lambda \mathcal{D}^T y_i)\big)$, for $i = 1, \ldots, n_c$;
4: $u^{k+1} \leftarrow \text{CNN}(\beta m^k)$;
5: $f^{k+1} \leftarrow \text{CNN}(\gamma \mathcal{F} u^{k+1})$;
6: $m^{k+1} \leftarrow \big((\beta+\gamma)I + \alpha \sum_{i=1}^{n_c} S_i^H S_i\big)^{-1}(\beta u^{k+1} + \gamma \mathcal{F}^{-1} f^{k+1} + \alpha \sum_{i=1}^{n_c} S_i^H x_i^{k+1})$;
7: **return** m, f

According to our Algorithm, we establish an end-to-end network structure as shown in Fig.1. The u-subproblem and f-subproblem are processed by convolutional neural network instead of hand-craft regularization terms. And this network is a residual network with a residual layer after CNN block. Fig.2 shows the CNN block which is composed of multiple convolution and activation layers. We stack the real and imaginary parts of the input into two-channel image to change complex value into real value. In this work, we use a simple network structure which can be replaced by more advanced networks such as U-Net [17] to improve the reconstruction effect, but this is not our focus.

Note that both x_i and m are updated by the corresponding Euler-Lagrange equation.We can obtain under-sampled multi-coil k-space data y_i and coil sensitivity S_i from the data, and estimate the masks D and under-sampled MR images m^0. The input m^k passes through a CNN block to obtain u^{k+1}, and then go by Fourier transform followed by another CNN block to obtain f^{k+1}. In addition, m^k and $S_i, \mathcal{D}, y_i$ are also taken as inputs to estimate x_i^{k+1}, which are integrated with u^{k+1} and f^{k+1} to obtain the output m^{k+1} as shown in Fig. 1.

III. Implementation and Experiments

A. Loss function

We use the following dual domain loss function to train the network

$$\mathcal{L}(\Theta) = \sum_{i=1}^{n_i} \left(\|m_i^{n_{it}}(\Theta) - g_i\|_2^2 + \|f_i^{n_{it}}(\Theta) - \mathcal{F} g_i\|_2^2 \right),$$

where n_i is the number of training images, and g_i is the reference image.This loss function expresses the difference between the reconstruction and the ground truth on the dual domain.

TABLE I: Experimental results of learning-based methods using different iterations (n_{it}) on Axial T2 dataset.

	$n_{it}=5$		$n_{it}=10$		$n_{it}=15$	
Method	PSNR	SSIM	PSNR	SSIM	PSNR	SSIM
VS-Net	39.06	**0.9565**	39.50	0.9583	39.65	**0.9582**
DVS-Net	**39.37**	0.9502	**39.94**	**0.9595**	**40.05**	0.9575

B. Dataset and training details

We use a public knee MR dataset[1] in [11] for evaluation. Each protocol contains 20 volumes with about 40 slices. The total number of receiver coils (n_c) is 15 and the coil sensitivities has been given. For each protocol, we take 19 volumes out of the 20 volumes to train the neural networks, and use the remaining one for testing. During training, we used the non-uniform Cartesian sampling method to down sample the original data, and combine the coil sensitivities to obtain the under-sampled MR image. Note that 24 lines in the central region are retained for each under-sampling volume.

Because the training data set is relatively small, we use five convolutions in the m-CNN block and three convolutions in

[1]https://github.com/VLOGroup/mri-variationalnetwork

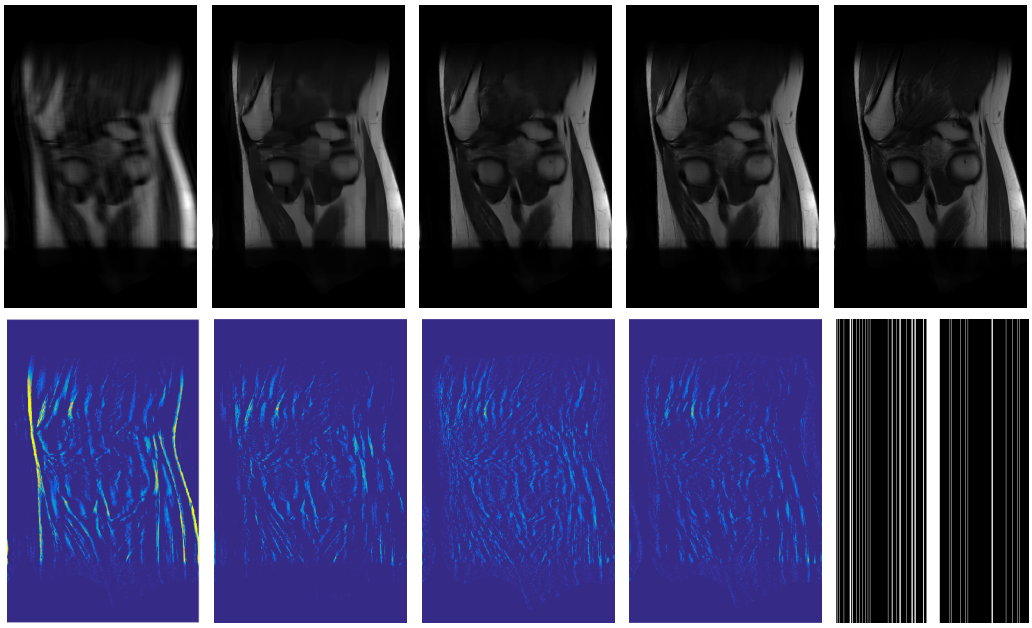

(a) Zero-filling (b) BM3D (c) VS-Net (d) DVS-Net (e) Reference/mask

Fig. 4: The visual comparison of four reconstruction methods on the Coronal PD dataset undersampled 6-fold.

TABLE II: Comparison results on four datasets obtained by Zero-filling, BM3D, VS-Net and DVS-Net.

	Axial T2		Coronal PD		Sagittal PD		Sagittal T2	
Method	PSNR	SSIM	PSNR	SSIM	PSNR	SSIM	PSNR	SSIM
Zero-filling	34.21	0.9325	30.95	0.8589	36.60	0.9495	35.98	0.9191
BM3D-MRI	37.23	0.9433	36.26	0.9099	41.05	0.9579	37.57	0.9135
VS-Net	39.50	0.9583	38.06	0.9299	42.71	**0.9738**	39.75	**0.9335**
DVS-Net	**39.94**	**0.9595**	**38.43**	**0.9310**	**43.15**	0.9736	**40.03**	0.9311

the f-CNN block to avoid over-fitting of the network during training process. We set the number of epoch to be 200 and batch size to be 1, and use Adam with learning rate 10^{-3} and decay rate 0.1 to optimize the networks.

C. Experimental results

We compare the performance of DVS-Net with zero-filling, BM3D-MRI [12] and VS-Net [10] for under-sampled parallel MRI data in a variety of situations, and use both Peak Signal to Noise Ratio (PSNR) and Structural Similarity (SSIM) to evaluate the quality of the reconstructed image. For the single-coil method BM3D-MRI, the under-sampled k-space data is reconstructed separately, and integrated together by combining the coil sensitivities. We retrain the VS-Net using the same parameter settings as suggested in the original papers.

On the first place, we evaluate DVS-Net and VS-Net with different numbers of iterations. As shown in Table I, the PSNR value of both the two methods increases as the iteration number n_{it} increases from 5 to 15, and the advantages of DVS-Net is very stable with different numbers of iterations. Fig.3 shows the change curves of three evaluation indicators in both training process and testing process when different iterations are selected. It can be seen that there is no over-fitting phenomenon, and the results of selecting 10 and 15 iterations are not much different and even tend to be the same on the test set. Therefore, we simply set $n_{it} = 10$ in the followings. Table II shows the quantitative evaluations among zero-filling, BM3D-MRI, VS-Net and DVS-Net on four protocols with 6-fold acceleration factors. The visual comparison on the Coronal PD dataset are displayed in Fig. 4. As can be seen, the learning-based methods outperform the BM3D-MRI method for all protocols, and DVS-Net outperforms VS-Net due to the joint dual domain reconstruction strategy.

Moreover, we degrade the two protocols by white Gaussian noises with mean 0 and standard deviation 0.005 and evaluate the learning based methods for both 6-fold and 8-fold acceleration factors. Table III provides the PSNR and SSIM on two protocol sagittal PD and T2, where the proposed dual domain reconstruction method always gives higher PSNR than the SOTA VS-Net. The visual comparison for the 8-fold T2 data are displayed in Fig.5. As shown by the residual images, DVS-Net presents less information than VS-Net, which also concur with the PSNR comparison.

IV. CONCLUSION

In this paper, we proposed a novel dual-domain reconstruction model to fully make use of information in frequency domain and image domain, where a data term on the frequency domain and image domain was introduced to maintain data consistency. In order to integrate the advances

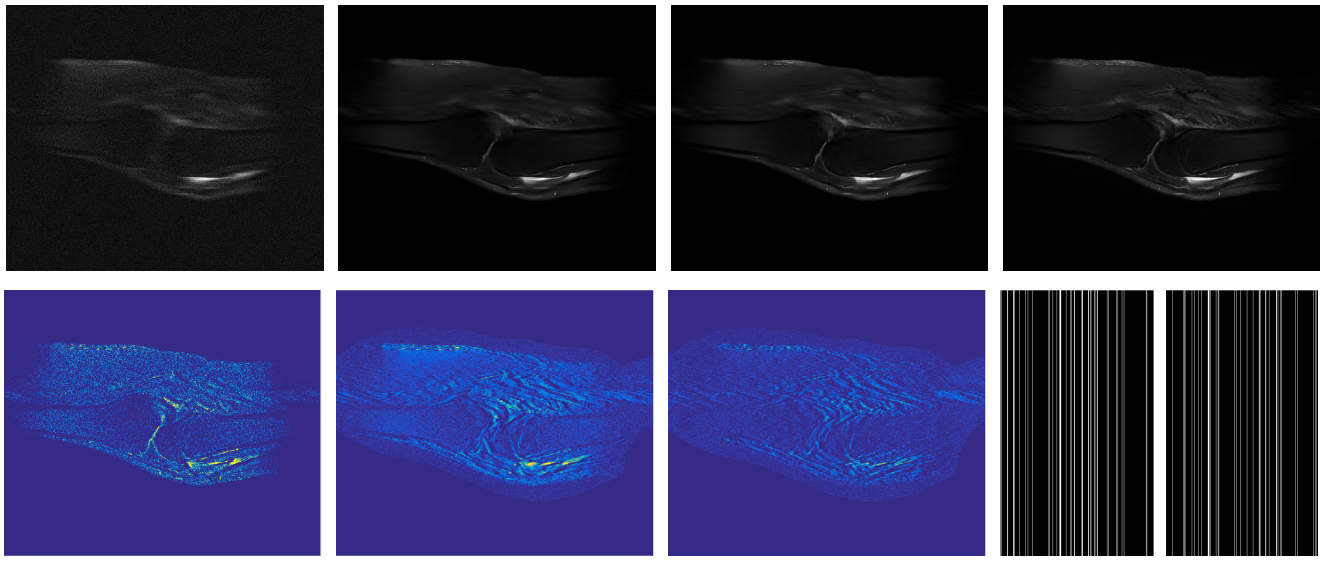

(a) Zero-filling (b) VS-Net (c) DVS-Net (d) Reference/mask

Fig. 5: The visual comparison of DVS-Net and VS-Net of the Sagittal T2 dataset with Gaussian noise undersampled 8-fold.

TABLE III: The comparison results obtained by the learning based methods when reconstructing noisy data, where 'acc' stands for the acceleration factor.

		acc=6		acc=8	
Protocol	Method	PSNR	SSIM	PSNR	SSIM
Sagittal PD	Zero-filling	23.04	0.1142	23.03	0.1124
	VS-Net	42.52	**0.9733**	41.28	**0.9679**
	DVS-Net	**42.98**	**0.9733**	**41.64**	0.9674
Sagittal T2	Zero-filling	25.14	0.1826	25.18	0.1831
	VS-Net	39.65	**0.9329**	39.07	**0.9267**
	DVS-Net	**40.03**	0.9324	**39.48**	0.9229

of both model-based and learning-based approaches, we implemented the ADMM to obtain an iterative algorithm, where the deep neural network was used to approximate the resolvent operators and gain an end-to-end trainable network. Numerical experiments on knee MR data were conducted to demonstrate that the dual-domain method can improve the reconstruction accuracy.

REFERENCES

[1] A. Deshmane, V. Gulani, M. A. Griswold, and N. Seiberlich, "Parallel mr imaging," *Journal of Magnetic Resonance Imaging*, vol. 36, no. 1, pp.55–72, 2012.

[2] T. Eo, Y. Jun, T. Kim, J. Jang, H.-J. Lee, and D. Hwang, "KIKI-net: cross-domain convolutional neural networks for reconstructing undersampled magnetic resonance images," *Magnetic Resonance in Medicine*, vol. 80,no. 5, pp. 2188–2201, Apr. 2018.

[3] R. Souza, R. M. Lebel, and R. Frayne, "A hybrid, dual domain, cascade of convolutional neural networks for magnetic resonance image reconstruction," in *Proceedings of The 2nd International Conference on Medical Imaging with Deep Learning*, vol. 102, 2019, pp. 437–446.

[4] W.-A. Lin, H. Liao, C. Peng, X. Sun, J. Zhang, J. Luo, R. Chellappa, and S. K.Zhou, "Dudonet: Dual domain network for ct metal artifact reduction," in *Proceedings of the IEEE/CVF Conference on Computer Vision and Pattern Recognition*, 2019, pp. 10 512–10 521.

[5] B. Zhou and S. K. Zhou, "Dudornet: Learning a dual-domain recurrent network for fast mri reconstruction with deep t1 prior," in *Proceedings of the IEEE/CVF Conference on Computer Vision and Pattern Recognition (CVPR)*, June 2020, pp. 4273–4282.

[6] W. Cheng, Y. Wang, Y. Chi, X. Xie, and Y. Duan, "Learned full-sampling reconstruction," in *International Conference on Medical Image Computing and Computer-Assisted Intervention*. Springer, 2019, pp. 375–384.

[7] W. Cheng, Y. Wang, H. Li, and Y. Duan, "Learned full-sampling reconstruction from incomplete data," *IEEE Transactions on Computational Imaging*, vol. 6, pp. 945–957, 2020.

[8] G. Liu, F. A. Reda, K. J. Shih, T.-C. Wang, A. Tao, and B. Catanzaro, "Image inpainting for irregular holes using partial convolutions," in *Proceedings of the European Conference on Computer Vision (ECCV)*, 2018, pp. 85–100.

[9] J. Cheng, H. Wang, L. Ying, and D. Liang, "Model learning: Primal dual networks for fast mr imaging," in *International Conference on Medical Image Computing and Computer-Assisted Intervention*. Springer, 2019, pp. 21–29.

[10] J. Duan, J. Schlemper, C. Qin, C. Ouyang, W. Bai, C. Biffi, G. Bello, B. Statton, D. P. O'regan, and D. Rueckert, "Vs-net: Variable splitting network for accelerated parallel mri reconstruction," in *International Conference on Medical Image Computing and Computer-Assisted Intervention*. Springer, 2019, pp. 713–722.

[11] K. Hammernik, T. Klatzer, E. Kobler, M. P. Recht, D. K. Sodickson, T. Pock, and F. Knoll, "Learning a variational network for reconstruction of accelerated mri data," *Magnetic resonance in medicine*, vol. 79, no. 6, pp. 3055–3071, 2018.

[12] E. M. Eksioglu, "Decoupled algorithm for MRI reconstruction using nonlocal block matching model: BM3d-MRI," vol. 56, no. 3, pp. 430–440, Mar. 2016.

[13] Y. Jun, H. Shin, T. Eo, and D. Hwang, "Joint deep model-based mr image and coil sensitivity reconstruction network (joint-icnet) for fast mri," in *Proceedings of the IEEE/CVF Conference on Computer Vision and Pattern Recognition*, 2021, pp. 5270–5279.

[14] H. Wang and J. Cheng, "Accelerating mr imaging via deep chambolle-pock network*," in *2019 41st Annual International Conference of the IEEE Engineering in Medicine and Biology Society (EMBC)*, 2019, pp. 6818–6821.

[15] Y. Nakagawa and D. Kokuryo, "Image reconstruction method with compressed sensing for high-speed mr temperature measurement of abdominal organs*," in *2019 41st Annual International Conference of the IEEE Engineering in Medicine and Biology Society (EMBC)*, 2019, pp. 2731–2735.

[16] K. Koolstra and R. Remis, "Learning a preconditioner to accelerate compressed sensing reconstructions in mri," *Magnetic Resonance in Medicine*, 2021.

[17] O. Ronneberger, P. Fischer, and T. Brox, "U-net: Convolutional networks for biomedical image segmentation," in *Medical Image Computing and Computer-Assisted Intervention – MICCAI 2015*, 2015, pp. 234–241.